https://doi.org/10.5194/hess-2019-586
Preprint. Discussion started: 17 March 2020

Hydrology and Earth System Sciences
Discussions
Open Access

A novel framework of deriving joint impoundment rules for large-scale reservoir system based on a classification-aggregation-decomposition approach

Shaokun He[1, 2, 3], Shenglian Guo[1, *], Chong-Yu Xu[1, 3], Kebing Chen[1], Zhen Liao[1], Lele Deng[1], Huanhuan Ba[1], Dimitri Solomatine[2, 3]

[1]State Key Lab. of Water Resources & Hydropower Engineering Science, Wuhan Univ., 430072, Wuhan, China;

[2]Hydro-informatics Group, IHE Delft Institute for Water Education, Delft, the Netherlands;

[3]Water Resources Sect., Delft Univ. Technol., Delft, the Netherlands;

[4]Dept. of Geosciences, University of Oslo, Oslo, Norway.

**Correspondence author*: *Shenglian Guo* (Email: slguo@whu.edu.cn).

Abstract: Joint and optimal impoundment operation of the large-scale reservoir system has become more crucial for modern water management. Since the existing techniques fail to optimize the large-scale multi-objective impoundment operation due to the complex inflow stochasticity and high dimensionality, we develop a novel combination of parameter simulation optimization and classification-aggregation-decomposition approach here to overcome these obstacles. There are four main steps involved in our proposed framework: (1) reservoirs classification based on geographical location and flood prevention targets; (2) assumption of a hypothetical single reservoir in the same pool; (3) the derivation of the initial impoundment policies by the non-dominated sorting genetic algorithm-II (NSGA-II); (4) further improvement of the impoundment policies via Parallel Progressive Optimization Algorithm (PPOA). The framework potential is performed on China's mixed 30-reservoir system in the upper Yangtze River. Results indicate that our method can provide a series of schemes to refer to different flood event scenarios. The best scheme outperforms the conventional operating rule, as it increases impoundment efficiency from 89.50% to 94.16% and hydropower generation by 7.70 billion kWh (or increase 3.79%) while flood control risk is less than 0.06.

Keywords: Large-scale reservoir system; Joint impoundment rules; Multi-objective operation; Classification-aggregation-decomposition; Yangtze River basin

1 Introduction

Rapid economic development and the growth of the human population are responsible for more serious and wider water-related challenges, which lead to greater stress on water resources management. One of the most effective measures to alleviate water issues is to regulate natural streamflow via reservoirs (Lauri et al., 2012;Ng et al., 2017). Cascade impoundment operation can properly achieve the goal since it stores excess water during the wet season and depletes reservoir storage during the dry season (Afshar et al., 2010;Labadie, 2004). In recent decades, impoundment operation has been one hot academic topic. Considerable research efforts (Liu et al., 2011;Paredes and Lund, 2006;Xu et al., 2017;Yeh, 1985) frequently point out that its key to the scientific operation is deriving effective operating policies. However, most of the literature merely focuses on the small-scale reservoir system, yet fails to address the complex inflow stochasticity and high dimensionality of the multi-objective trans-basin (Yan et al., 2012) and trans-province impoundment problems (Jurasz and Ciapala, 2017), even if the latter large-scale impoundment operation is more necessary and suitable for

https://doi.org/10.5194/hess-2019-586
Preprint. Discussion started: 17 March 2020

modern water resources management (Wang et al., 2014;Zhou et al., 2018).

As a matter of fact, the inherent scientific characteristics of inflow stochasticity for large-scale impoundment operation has no difference with the small-scale one, there are three theoretical breakthroughs to cope with it: (1) implicit stochastic optimization (ISO) (Feng et al., 2017), (2) explicit stochastic optimization (ESO) (Goor et al., 2010), and (3) parameter simulation optimization (PSO) (Zhang et al., 2019). ISO requires 'perfect inflow forecast' and ESO behaves in a more complex way to explicitly incorporate all inflow probabilities. PSO is relatively preferred for large-scale operation (Celeste and Billib, 2009;Tan et al., 2017), which predefines a rule curve shape and then employs heuristic algorithms to identify the best parameter combination under all possible inflow scenarios. Regarding another well-known 'high dimensionality' in the PSO framework, the original simulation model is usually replaced by a surrogate model for simplification. The surrogate should preserve and describe the main features of the original model (Chu et al., 2015;Shaw et al., 2017;Zhang et al., 2017). The subtle combination of the PSO framework and a surrogate model has indeed made some achievements in addressing inflow stochasticity and dimensional curse of multi-reservoir hydropower (Glotic and Zamuda, 2015;Valdes et al., 1992) and flood control operations (Zhang et al., 2019), but is seldom utilized in large-scale impoundment operation.

The major challenge lies in the reliability of the surrogate model. On the one hand, it should highlight the reservoir storage state as the most vital indicator to track the original system status, since the highest priority of impoundment operation is to ensure certain storage for flood prevention during the operating horizon and to raise enough end reservoir storage for water demand during the following dry period (Li et al., 2018;Xu et al., 2017); Additionally, it also should reduce the number of decision variables, making it possible to solve the curse of dimensionality. While it is noticed that reservoirs can be classified into different pools according to the tributaries and flood prevention targets (Zhang et al., 2014), a novel idea of 'classification-aggregation-decomposition' is naturally introduced to structure the proper surrogate model. The reservoirs in the same pool are firstly aggregated in water units to capture reservoir storage information, then a decomposition method is used to decentralize reservoir storage decisions into individual reservoirs in each pool. The salient feature of this approach is to simplify the large-scale system into several equivalent hypothetic reservoirs via aggregation, which caters to the replacement requirement of the impoundment model.

Nevertheless, the current decomposition methods still have some degree of drawbacks. Li et al. (2014a) and Zhang et al. (2019) allocated the virtual reservoir output to individual reservoirs by using the empirical equations. Both made a quick decision on decomposition forms but did not consider the maximum utilization of water resources. Tan et al. (2017) adopted an improved genetic algorithm to seek for the optimal decomposition scheme in the water-supply systems, but it is more time-consuming since the calculation of the evaluation function goes to an exponential increase with the number of involved reservoirs (Castelletti et al., 2012;Zhao et al., 2012). These common techniques cannot balance computing efficiency and optimal operating rules well. This limits their further application in practice. Actually, the recent implementation of parallel computation has been proved able to reach a balance point (Li et al., 2014b;He et al., 2019), although the parallelization technique attracts little attention up to now. To this end, an emerging method-Parallel Progressive Optimization Algorithm (PPOA) (Feng et al., 2018b) is introduced to assist our decomposition strategy. It is a means of improving the quality of optimization while using a multi-core configuration to enhance execution efficiency (Cheng et al., 2014).

To verify the feasibility of the proposed framework, we select a typical mixed 30-reservoir system in China as the case study, where two objectives of reservoir impoundment efficiency (*IE*) and flood control risk (*FCR*) are simultaneously optimized, and then PPOA improves hydropower generation of individual reservoirs of each pool without *IE* and *FCR* distortion. The remainder of the paper is structured as follows: Section 2 addresses the 30-reservoir system and describes their conventional operating rules for impoundment operation; Section 3 introduces the framework in detail; Section 4 and Section 5 provide the experimental results and the application prospects of this method; Section 6 ends with the conclusions.

2 Case study

The Yangtze River (in Fig. 1a) basin possesses abundant water potential in China. It drains a catchment of 1.80 million km^2 with a total length of 6,300km. Its main tributaries include the Jinsha River, Yalong River, Min River, Jialing River, and Wu River. Owing to the subtropical monsoon climate, the Yangtze River basin often suffers from the uneven temporal and spatial distribution of flood hazards induced by heavy

https://doi.org/10.5194/hess-2019-586
Preprint. Discussion started: 17 March 2020

rainfalls. A series of large reservoirs have been built along its mainstream and tributaries to allocate water resources in recent decades. Among them, a 30-reservoir system including the core Three Gorges Reservoir (TGR) (in Fig. 1b) is one of the most critical water conservancy projects in China. Most reservoirs in the system serve multi-purposes (e.g., flood control, energy generation, tourism), except for Ge-Zhou-Ba (GZB) which is a run-of-river hydropower station. Particularly, TGR serves as the largest water project around the world, which is not only equipped with 22.50 GW installed hydropower capacity, but also prevents downstream flood disaster. The 30-reservoir system usually implements an impoundment operation to develop water resources. The characteristic parameters of the 30 reservoirs are shown in Table 1.

<Please insert Fig. 1 here>

<Please insert Table 1 here>

For the impoundment operation of these reservoirs, Conventional Operating Rules (CORs) are often individually predefined at the planning stage of reservoir construction to provide guidelines. As Fig. 2 shows, COR suggests that the reservoir water level should rise linearly throughout the whole impoundment horizon until it is up to the top of the conservation pool. However, overlapping the impoundment time of cascade reservoirs makes them compete with each other. It results in reduced water supplies to face the following non-flood season. In fact, two preset strategies of (1) advancing initial impoundment operation timing, but not earlier than Aug 1st; (2) raising the reservoir water levels, can be activated to excavate the potential benefits of joint impoundment operation on China's reservoir communities in the upper Yangtze

https://doi.org/10.5194/hess-2019-586
Preprint. Discussion started: 17 March 2020

River basin (He et al., 2019). The aim of the joint impoundment operation of the 30-reservoir system is to make efficient water resources utilization, on the condition that it reserves enough storage capacity for flood control. The restored inflow series from Aug 1st to Dec 31st spanning over 57 years (i.e. 1956-2012) are collected from the Yangtze River (Changjiang) Water Resources Commission. The time step used is ten (or eleven) days, a traditional Chinese measure of time, and therefore there are 15 operating periods for the five months per year.

<Please insert Fig. 2 here>

3 Methodology

Fig. 3 shows our research framework to derive the optimal impoundment rules for the 30-reservoir system. The methodological modules are summarized below:

(1) All reservoirs are classified into different pools (in Table 1) according to their geographic locations and flood prevention targets etc.;

(2) Reservoirs in the same pool are aggregated in water units to be a virtual reservoir and the virtual reservoir storage is treated as the state variable during the optimization process;

(3) PSO is employed to derive initial impoundment rules by considering the trade-offs between *IE* and *FCR*;

(4) PPOA helps formulate the final impoundment rules by boosting hydropower generation without *IE* and *FCR* distortion.

<Please insert Fig. 3 here>

3.1 Reservoirs classification

https://doi.org/10.5194/hess-2019-586
Preprint. Discussion started: 17 March 2020

Hydrology and Earth System Sciences Discussions
Open Access

During an impoundment optimization process, the dimensionality of decision variables increases linearly with the number of reservoirs; meanwhile, the computational burden of the objective function trends an exponential increase (Galelli and Castelletti, 2013). The vast reservoir community results in 'dimensionality disaster', which makes it tricky to derive effective joint rules. An attractive alternative to solve dimensionality restrictions is to classify these reservoirs and reduce their decision variables. The basic idea is to divide the 30-reservoir system into different pools according to their geographic distributions in the same tributary and flood prevention targets etc. (Heever and Grossmann, 2000;Saad et al., 1994).

3.2 Aggregation and decomposition schemes

Conceptually, these reservoirs in the same pool can be assembled into a virtual one. The hypothetical reservoir should retain the main characteristics yet ignore its hydraulic connection (Duran et al., 1985). As shown below, the reservoirs are aggregated in water units to simplify guidance on impoundment optimization (Tan et al., 2017):

$$V_i^*(t)=\sum_{n=1}^{M_i}V_{i,n}(t) \tag{1}$$

$$I_i^*(t)=\sum_{n=1}^{M_i}I_{i,n}(t)-Eva_i(t) \tag{2}$$

where $V_i^*(t)$ and $I_i^*(t)$ are hypothetical reservoir storage and inflow of the ith pool at time t, respectively; $V_{i,n}(t)$ and $I_{i,n}(t)$ are the storage and inflow from external sources of the nth reservoir of the ith pool at time t, respectively; $Eva_i(t)$ is the sum loss of the ith pool at time t (e.g., evaporation, seepage); M_i is the total number of reservoirs in the ith pool.

https://doi.org/10.5194/hess-2019-586
Preprint. Discussion started: 17 March 2020

As reservoir storage is often treated as the state variable for reservoir operation (Feng et al., 2018a;Chang and Chang, 2006), the virtual storage $V_i^*(t)$ is chosen here as the state variable for the optimization process. It can be easily formulated by Eq. (1) in any case of reservoir topology (shown in Fig. 4). Fig. 4(a) and Fig. 4(b) are considered in our case study.

<Please insert Fig. 4 here>

The state variable $V_i^*(t)$ of each pool at all periods could be determined by the aggregated impoundment rules. Another issue is how to allocate $V_i^*(t)$ to individual reservoirs in the same pool. Some traditional decomposition strategies (e.g., fixed proportions) have been experimented well (Turgeon, 1980;Zhang et al., 2019). In our study, a similar decomposition way of the percentage of the allowable reservoir storage is initially taken:

$$V_{i,n}(t) = SL_{i,n}(t) + (V_i^*(t) - \sum_{m=1}^{M_i} SL_{i,m}(t)) \times \frac{SS_{i,n}(t) - SL_{i,n}(t)}{\sum_{m=1}^{M_i}(SS_{i,m}(t) - SL_{i,m}(t))} \quad (3)$$

where $SL_{i,n}(t)$ is the lower boundary of the nth reservoir storage of the ith pool at time t; $SS_{i,n}(t)$ is the nth reservoir storage of the ith pool at time t, which is relative to its seasonal top of buffer pool.

3.3 Parameter simulation optimization (PSO)

The decomposition structure is embedded into the aggregation module, where the latter combines with the multi-objective impoundment model to explore trade-offs between the *IE* maximization and the *FCR* minimization (Liu et al., 2011;Zhou et al., 2015). We established the PSO framework (Giuliani et al., 2016;Celeste and Billib, 2009) here to identify the initial impoundment strategies. As there are seven pools for

https://doi.org/10.5194/hess-2019-586
Preprint. Discussion started: 17 March 2020

the 30-reservoir system and 15 decision variables for each virtual reservoir (one decision variable corresponds to one operating period), there are a total of 105 (=7*15) decision variables for these seven virtual reservoirs rather than 450 (=30*15) decision variables in real.

3.3.1 Objective functions and constraints

IE is a critical indicator for impoundment operation to assess water resources potential in the case of controllable *FCR* (Zhou et al., 2018):

(1) *IE* represents future water resources utilization for the following non-flood period, it can be defined as follows:

$$max\ \ IE = \frac{1}{Y}\sum_{y=1}^{Y}\frac{\sum_{i=1}^{I}\sum_{n=1}^{M_i}(VE_{i,n}(y)-SD_{i,n})}{\sum_{i=1}^{I}\sum_{n=1}^{M_i}(SU_{i,n}-SD_{i,n})} \tag{4a}$$

$$IE_{i,n} = \frac{1}{Y}\sum_{y=1}^{Y}\frac{VE_{i,n}(y)-SD_{i,n}}{SU_{i,n}-SD_{i,n}} \tag{4b}$$

where $IE_{i,n}$ is the annual impoundment efficiency of the *n*th reservoir of the *i*th pool; $VE_{i,n}(y)$ is the end storage of the *n*th reservoir of the *i*th pool in the *y*th year; $SU_{i,n}$, and $SD_{i,n}$ is the *n*th reservoir storages of the *i*th pool, which corresponds to their top of conservation pool and inactive pool, respectively. *I* and *Y* are the number of all pools and years, respectively. *I* is 7 in our case.

(2) *FCR*, another critical objective to control the impoundment process, can be evaluated as follows:

$$min\ \ FCR = min\ \{max\ \{FCR(t)\}\},\quad (0 < t \le T \cdot Y) \tag{5a}$$

$$FCR(t) = max\{\frac{\sum_{i=1}^{I}\sum_{n=1}^{M_i}(V_{i,n}(t) - SS_{i,n}(t))}{\sum_{i=1}^{I}\sum_{n=1}^{M_i}(SU_{i,n} - SS_{i,n}(t))}, 0\} \tag{5b}$$

$$FCR_{i,n}(t) = max\{\frac{V_{i,n}(t) - SS_{i,n}(t)}{\sum_{i=1}^{I}\sum_{n=1}^{M_i}(SU_{i,n} - SS_{i,n}(t))}, 0\} \tag{5c}$$

where $FCR_{i,n}(t)$ is the FCR of the nth reservoir of the ith pool at time t; T is the number of operating periods in one year.

3.3.2 Constraints

A reservoir operation model generally contains the following constraints:

(1) Mass balance equation:

$$V_{i,n}(t+1) = V_{i,n}(t) + (I_{i,n}(t) + \sum_{j \in \Phi_{j,i,n}} R_j(t) - R_{i,n}(t)) \cdot \Delta t \tag{6}$$

(2) Reservoir storage limits

$$SL_{i,n}(t) \le V_{i,n}(t) \le SS_{i,n}(t) \tag{7}$$

(3) Water discharge limits

$$RL_{i,n}(t) \le R_{i,n}(t) \le RU_{i,n}(t),\ \ R_{i,n}(t) = Q_{i,n}(t) + QS_{i,n}(t) \tag{8}$$

(4) Hydropower generation limits

$$PL_{i,n}(t) \le N_{i,n}(t) \le PU_{i,n}(t) \tag{9}$$

(5) Boundary conditions

$$Z_{i,n}(t) = \begin{cases} Z_{i,n,begin},\ t = 1, T+1, ..., (Y-1)T+1 \\ Z_{i,n,end},\ t = T, 2T, ..., YT \end{cases} \tag{10}$$

where

$V_{i,n}(t), V_{i,n}(t+1)$	the nth reservoir storage of the ith pool at the beginning and end time t
$\Phi_{j,i,n}$	the upstream reservoir set which has a physical connection with the nth reservoir of the ith pool
$I_{i,n}(t)$	the nth reservoir inflow of the ith pool from external sources at time t

https://doi.org/10.5194/hess-2019-586
Preprint. Discussion started: 17 March 2020

$R_{i,n}(t)$	the *n*th reservoir release of the *i*th pool at time *t*
Δt	the time interval, day
$SL_{i,n}(t), SS_{i,n}(t)$	the lower and upper storage boundaries of the *n*th reservoir of the *i*th pool at time *t*
$RL_{i,n}(t), RU_{i,n}(t)$	the lower and upper water release boundaries of the *n*th reservoir of the *i*th pool at time *t*
$Q_{i,n}(t)$	the generation discharge of the *n*th reservoir of the *i*th pool at time *t*
$QS_{i,n}(t)$	the spillway water of the *n*th reservoir of the *i*th pool at time *t*
$PL_{i,n}(t), PU_{i,n}(t)$	the lower and upper hydropower output boundaries of the *n*th reservoir of the *i*th pool at time *t*
$Z_{i,n}(t)$	the water level of the *n*th reservoir of the *i*th pool at time *t*
$Z_{i,n,begin}$, $Z_{i,n,end}$	the annual top of buffer pool and top of conservation pool of the *n*th reservoir of the *i*th pool

3.3.3 Optimization algorithm

The NSGA-II algorithm (Deb et al., 2002) has made some successful achievements in the PSO work of the reservoir field (Lei et al., 2018;Lotfan et al., 2016). It realizes a fast convergence in Pareto frontiers with the crowding distance and the non-dominated sorting rank (Deb et al., 2002). NSGA-II is implemented in this paper, even if some other heuristic algorithms may also be able to handle it. The experimental parameter is set as: the population size = 64, generation = 100, cross-over probability = 0.9 and mutation rate = 0.1.

3.4 Coordination model

The above procedures could realize a quick impoundment policy but fail to make further water resource utilization. Finally, yet importantly, the problem is how to excavate water potential.

3.4.1 Objective function and constraints

https://doi.org/10.5194/hess-2019-586
Preprint. Discussion started: 17 March 2020

For large-scale impoundment operations in China, reservoir release usually generates hydropower and then is transmitted to water consumers. As *IE* and *FCR* occupy the highest priority, hydropower has to comply with the impoundment rules. A good impoundment rule is to ensure that the impoundment quality of the reservoir is achieved besides maximizing hydropower generation.

To this end, the corresponding coordination model is introduced below, which maximizes the annual hydropower generation of the *i*th pool (E_i):

$$max\ E_i = \frac{1}{Y}\sum_{n=1}^{M_i}\sum_{t=1}^{T\cdot Y} N_{i,n}(t)\cdot\Delta t,\ \ N_{i,n}(t) = A_{i,n}Q_{i,n}(t)H_{i,n}(t) \tag{11}$$

where $A_{i,n}$ is the power coefficient of the *n*th reservoir of the *i*th pool; $H_{i,n}(t)$ is the powerhead of the *n*th reservoir of the *i*th pool at time *t*; other symbols refer to Section 3.3.2.

Except for the constraints described in Section 3.3.2, the additional constraints in Eq. 12 and Eq. 13(a-b) for each pool must be met during the whole period.

$$IE_i = \frac{1}{Y}\sum_{y=1}^{Y}\frac{\sum_{n=1}^{M_i}(VE_{i,n}(y) - SD_{i,n})}{\sum_{n=1}^{M_i}(SU_{i,n} - SD_{i,n})} \ge IE_i^* \tag{12}$$

$$FCR_i \le FCR_i^* \tag{13a}$$

$$FCR_i = max\{\frac{\sum_{n=1}^{M_i}(V_{i,n}(t) - SS_{i,n}(t))}{\sum_{n=1}^{M_i}(SU_{i,n} - SS_{i,n}(t))}, 0\},\ \ (0 < t \le T\cdot Y) \tag{13b}$$

where initial IE_i^* and FCR_i^* of the *i*th pool are determined by Pareto Frontier in the PSO framework.

3.4.2 Parallel progressive optimization algorithm (PPOA)

Recently, PPOA (Feng et al., 2018b) has emerged as a means of improving initial

https://doi.org/10.5194/hess-2019-586
Preprint. Discussion started: 17 March 2020

solution quality. It can use abundant multi-core configuration to improve execution efficiency while keeping the performance of the standard progressive optimization algorithm (POA). The details of PPOA can be further referred to in other literature (Feng et al., 2018b;Xie et al., 2015). Here is illustrated as an example of PPOA with 3-reservoir and 3 levels per reservoir (in Fig. 5). Fig.5 shows that all the calculations of the 27 (=3^3) state combinations are completely independent of each other for a single sub-problem. In other words, the fitness value of any one state combination has no influence on other state combinations, which reveals the good parallelism features. PPOA adopts a successive approximation strategy to gradually improve solution quality, which will make more sense with the dimensional expansion.

<Please insert Fig. 5 here>

4 Results

4.1 Pareto Frontiers of NSGA-II between *IE* and *FCR*

With the help of the NSGA-II algorithm, a wide array of Pareto Frontier is explored within allowable impoundment storage capacity (in Table 2) and subsequently, *COR* serves as the benchmark. The initial *IE* and *FCR* values of the extensively distributed Pareto Frontier and the *COR* result for the whole research basin are visualized in Fig. 6.

<Please insert Table 2 here>

<Please insert Fig. 6 here>

Fig. 6 shows that the improvement of one objective is bound to be followed by the sacrifice of another objective. But these Pareto Frontiers still are able to adjustably counterbalance *IE* and *FCR* simultaneously. More specifically, the optimal initial *FCR* solution (Solution ① in Fig. 6) can be considered while a wet inflow scenario during the impoundment horizon is predicted in advance; on the contrary, the optimal initial *IE* solution (Solution ③ in Fig. 6) could be more appropriate in a dry impoundment scenario; at the end, the compromised initial solutions can be competent for different impoundment scenarios with medium-scale inflow hydrograph.

We use the universal projection pursuit method (PP) (Friedman, 1987;He et al., 2020) to evaluate the quality of all the Pareto Frontiers. PP can transform the 2-dimensional values (*IE* and *FCR* values) to one-dimensional data with the help of the projection vector and rank all solutions according to the one-dimensional value. Because the possibility of large-scale flood events decreases over impoundment time, these Pareto solutions with latter *FCR* appearance time are more preferred by decision-makers. Finally, the Pareto Frontier (whose *IE* and *FCR* values are 94.16% and 0.06, respectively) is selected as the initial optimal solution (Solution ② in Fig. 6). Solution ① and ③ are also included in the next sections, as Solution ① always produces much higher *IE* than COR when there is no flood control risk (*FCR* = 0); Solution ③ makes a better deal with joint impoundment operation in dry scenarios when the influence of flood control can be ignored.

4.2 Optimal results of the final impoundment policies

We improved these three alternatives (i.e., Solution ①, ②, and ③) by the PPOA and obtained the final three representative impoundment policies (I, II and III) accordingly.

4.2.1 Behavior performance between *IE* and *FCR*

The relationships between *IE* and *FCR* of the impoundment policies I, II, III as well as COR for each of the 30 reservoirs are shown in Fig.7. Fig. 7 can easily distinguish the numerical changes (i.e. the *IE* and *FCR* increment) of reservoirs. For example, Reservoir D4 occupies the maximum *IE* value of 99.78% and Reservoir G1 occupies the maximum *FCR* value of 0.13. For Reservoir D4 with the maximum *IE*, it illustrates that there is enough inflow in pool D to contribute to its small impoundment storage, but upstream reservoirs with larger impoundment storage (Reservoirs D2 and D3) in the same pool are difficult to fill up, even if their *FCR* value slightly increase. Reservoir G1 has the maximum *FCR* value because Pool G fails to regulate massive water from the upstream tributaries and large interval catchment area. Reservoir G1 also has an ideal *IE* result yet leaves inadequate storage to control flood risk, once it activates the pre-set principle of raising the reservoir water level. In addition, it is obvious that under the benchmark of COR, some of the other reservoirs can get better *IE* improvement with a little or no *FCR* increase. For example, when the optimal impoundment policy I is adopted, the *IE* increase of the four reservoirs in pool C varies from 1.41% to 11.84%, while flood control standard remains unchanged (*FCR* is still 0). This means that: (1) these two pre-set strategies can have only positive effects on impoundment operation when they are reasonably regulated; (2) the larger the required impoundment storage of a reservoir, the better the potential impoundment prospect. The sharp *IE* improvement of Reservoir G1 with the largest impoundment storage further proves it. Reservoir G1 increases *IE* from 85.66% of COR to 94.64% of the impoundment policy I (i.e. 1.99 billion m^3 increment of impoundment storage). By

https://doi.org/10.5194/hess-2019-586
Preprint. Discussion started: 17 March 2020

contrast, the *IE* increment of reservoirs in pool A (except for Reservoir A6) and pool B is relatively less, where these reservoirs with smaller impoundment storage are operated by just lifting water level but remaining the initial impoundment timing unchanged.

<Please insert Fig. 7 here>

Fig. 7 also contains other significant information. Pools A, B, and F are not sensitive to *FCR*. Their maximum *FCR* values are still 0 under our proposed impoundment policies. It implies that these pools have enough flood control storage to deal with relatively easier flood control tasks. With the implement of the impoundment policy III, the other four investigative pools (C, D, E, and G) suffers from different degrees of flood control risk, especially Reservoir G1 (*TGR*) in pool G. Aiming at *FCR* varieties of Reservoir D2, D3 and D4 (in the same tributary) which are equipped with synchronous impoundment operations (i.e. all the impoundment timings start at Sep. 20th and end on Oct. 31st), it shows that the maximum *FCR* value decreases from upstream to downstream. The geographic elevations of these reservoirs have a substantial influence on their *FCR* distribution with the impact of spare reservoir storage. When runoff flows along cascade reservoirs, the upstream reservoir gives priority to storage volumes increment to lift water levels, which causes a decrease of downstream reservoir inflow. Consequently, the maximum *FCR* value of the downstream reservoir can be obviously reduced. Nevertheless, with the staggered impoundment time, these *FCR* values (e.g., Pool C) do not follow the principle of sequential decrease of Pool D. The *FCR* varieties of these reservoirs equipped with asynchronous impoundment operations in the same pool are more complicated to be analyzed.

4.2.2 Impact of optimal impoundment policies on hydropower generation

In this study, hydropower generation is the only indicator to assess water resource utilization of each pool. It is necessary to analyze the impact of the optimal impoundment policies on hydropower generation with comparison to COR. For the COR rule, the total simulated hydropower of the seven pools is 203.3 billion kWh. The top three are Pool C, G, and A, whose proportions are 43.04%, 20.78% and 14.18% (in Fig. 8), respectively. The sum of them is more than 75%. Hence, these three pools should be more focused when the PPOA algorithm coordinates individual reservoirs.

<Please insert Fig. 8 here>

We set the maximum number of iterations of the PPOA algorithm for Pool A, C, and G larger than other pools. Fig. 9 gives the hydropower generation results of seven pools with three different impoundment rules. It indicates that the optimal impoundment rules I, II and III can increase hydropower generation of the COR rule by 3.11%, 3.79%, and 3.89%, respectively. The top three growth rates are Pool G, C, and A. Especially, we can realize the huge potential hydropower of Pool G as its growth rate ranging from 5.26% to 7.41%. The reason owes to that Pool G possesses abundant water resources, where Reservoir G1 (TGR) is the largest hydropower plant in the word and Reservoir G2 (GZB) is one run-of-river hydropower plant. They can generate hydropower by converting kinetic energy into electricity more efficiently. Pool C can also increase hydropower by 3.27%~4.07%. It increases so much hydropower outputs because its four reservoirs located along the mainstream of the Yangtze River are

https://doi.org/10.5194/hess-2019-586
Preprint. Discussion started: 17 March 2020

equipped with large installed hydropower capacity (47.81 GW in total, see Table 1), thereinto, Reservoir C2 (BHT) is the second-largest hydropower station in China. However, the growth rates of hydropower of the other five pools are not obvious, even if there are six reservoirs in Pool A and seven reservoirs in Pool G. They stay low efficiency from potential energy to electricity, since they store limited water resources for future use.

<Please insert Fig. 9 here>

Moreover, Fig. 10 visualizes the hydropower increment of each pool in different streamflow scenarios (assumed that one year represents one scenario). It shows more hydropower details. It can be inferred that the optimal impoundment policy II is more suitable for all scenarios in comparison with the impoundment I or III. Policy II and III tap more hydropower potential of Pool C, G than I, but the flood control risk of II is smaller than III. The hydropower increments of Pool A for policy II level off, which illustrates that its impoundment rule is suitable for all the (wet, normal and dry) scenarios. The hydropower increments of Pool B, D, E, and F incur a negative loss in several dry scenarios, despite their annual average output present an increase. The slight adverse changes in these dry years are due to when the upstream reservoirs in these pools need more water to fill up their impoundment storage, the negative effect of the reduced generation discharge overweight the positive effect of the raising water head in the same time.

In addition, the hydropower growths of Pool C and G vary greatly with scenarios. It further reveals that due to the complex hydraulic connections among the pools, the single impoundment rule of Pool C and G cannot deal with all scenarios.

<Please insert Fig. 10 here>

4.3 Other evaluation indicators

Advanced joint impoundment operation will not only enhance water supply and hydropower generation but also make other benefits including economy, CO_2 emission reduction and so on, since it involves many factors directly or indirectly related to impoundment efficiency (Zhou et al., 2018). Here we present the boxplot of the outflow of all the seven pools (A~G) during the impoundment horizon to reveal its positive influence on downstream.

Fig. 11 intuitively shows that the optimal impoundment policy II can improve downstream streamflow requirements by altering its outflow distribution. For example, it keeps the minimum downstream streamflow in Pool G no lower than 8000 m^3/s in order to meet ecological needs, but the COR rule fails to satisfy this requirement in some dry scenarios. Moreover, it ensures downstream streamflow no higher than 39,900 m^3/s for downstream flood control in most years and 54,000 m^3/s for its own flood control safety in a few wet scenarios. It still behaves well than the COR rule to alleviate pressure on downstream flood control, where its maximum downstream streamflow is lower than that of the COR rule.

<Please insert Fig. 11 here>

5 Discussion

Due to the classification-aggregation-decomposition approach we put forward in this study, the novel framework of deriving joint impoundment rules can effectively

https://doi.org/10.5194/hess-2019-586
Preprint. Discussion started: 17 March 2020

overcome the tricky ‘curse of dimensionality’. In order to explore the computational efficiency of this method, we work in a Matlab environment equipped with a Windows system (Intel^{R} Core^{TM} i5-4590 CPU @ 3.30 GHz and 8.00 GB of RAM) and list the results of calculation time for different numbers of pools (shown in Fig. 12). Fig. 12 indicates that computational time increases with the number of pools, but does not increase exponentially with the number of reservoirs. It owes to the fact that in our method, the number of decision variables depends on the number of pools rather than the number of reservoirs. Its outstanding performance will become more prominent as the scale of the research reservoir is expanded. More specifically, time increases from 499 seconds to 8448 seconds when the number of reservoirs is from 6 to 30, which provides new possibilities for optimizing the so vast reservoir community in 10-days timescale. But actually, our proposed method can also optimize the daily impoundment operation of the mixed 30-reservoir system by taking about 39700 seconds (almost 11 hours), when we make several experiments assuming that daily runoff value of each reservoir can be discretized to be the same as its 10-day (11-day) runoff value.

<Please insert Fig. 12 here>

In addition, the novel method also inherits the inherent advantages of the multi-objective optimization algorithm (NSGA-II here). Aiming at multi-objective reservoir management, it not only produces the most optimal solutions as we referred to in Section 4 but also generates a series of optimal strategies that can compromise well on each objective. In our case, it gives rise to the operational alternatives available to decision-makers in terms of the *IE* results.

https://doi.org/10.5194/hess-2019-586
Preprint. Discussion started: 17 March 2020

Last but not least, we have to emphasize the benefits due to the introduction of the PPOA mechanism. Compared to the final optimization results of traditional decomposition strategies (i.e. Eq. (3)) (Zhang et al., 2017;Zhang et al., 2019), this method can use PPOA to boost hydropower generation of the mixed 30-reservoir system without *IE* and *FCR* distortion. The results between impoundment policies (I, II and II) and the traditional optimal solutions (①, ②, and ③) are compared. The final optimal *IE* and *FCR* results of impoundment policy I, II, III are 93.47% and 0, 94.16% and 0.06, 94.22% and 0.14, respectively. It can be seen that the *FCR* value can further be reduced (e.g., *FCR* of III is 0.14, less than that of Solution ③, 0.18). However, all three policies increase hydropower generation to varying degrees: 209.65 billion of I vs 206.34 billion of ①, 211.02 billion of II vs 208.77 billion of ②, and 211.22 billion of III vs 208.98 billion of ③. It also has a positive reference on future work of large-scale flood control and hydropower operations.

6 Conclusions

This study attempts to structure an adept framework of deriving joint impoundment rules, in which the classification-aggregation-decomposition and parameter-simulation-optimization approach are coupled to deal with the complex inflow stochasticity and high dimensionality in the large-scale cascade reservoirs, and then PPOA algorithm further improves the performance of operating rules. With a case study of the mixed 30-reservoir system in the upper Yangtze River, some vital conclusions are summarized below:

(1) A large number of reservoirs can be classified into several pools and the

https://doi.org/10.5194/hess-2019-586
Preprint. Discussion started: 17 March 2020

Hydrology and Earth System Sciences Discussions
Open Access

reservoirs in the same pool can be assembled to be an equivalent hypothetical reservoir. It proves another feasible pathway to overcoming the classical dimensionality issue in such a giant impoundment system via reducing decision variables.

(2) The multi-objective evolutionary algorithm coupled with the classification-aggregation-decomposition approach has powerful capabilities for the complicated cascade impoundment operation. With the help of the NSGA-II algorithm, the widely distributed Pareto Frontiers enable water resources managers to favorably decide the appropriate initial operating policies for a perfect compromise among the conflicting objectives.

(3) The PPOA method can help further increase hydropower generation of each pool without *IE* and *FCR* distortion. In comparison to the COR rule, our selected optimal impoundment rule can increase reservoir impoundment efficiency from 89.50% to 94.16% and hydropower generation by 7.70 billion kWh (or increase 3.79%) while the flood control risk is less than 0.06.

Data availability

The inflow data and reservoir characteristics parameters of the 30-reservoir system can be accessed by writing to the authors and filling a non-disclosure agreement under certain conditions.

Author contributions

SLG and SKH conceived the original idea, and they designed the methodology.

https://doi.org/10.5194/hess-2019-586
Preprint. Discussion started: 17 March 2020

SKH and KBC collected the data. SKH developed the model code and performed the simulations, with some contributions from ZL, LLD, and HHB. SKH wrote the paper, SLG, CYX, and DS revised the paper.

Competing interests

The authors declare that they have no conflict of interest.

Acknowledgments

We would like to thank the Yangtze River Commission for providing research data for the reservoir community.

Financial support

Our sincere gratitude goes to the fundings from the National Key Research and Development Plan (NO. 2016YFC0402206) of China, the National Natural Science Foundation of China (NO. 51879192, NO. 51879194) and China Scholarship Council (CSC).

https://doi.org/10.5194/hess-2019-586
Preprint. Discussion started: 17 March 2020

Reference

Afshar, A., Zahraei, A., and Marino, M. A.: Large-scale nonlinear conjunctive use optimization problem: decomposition algorithm, J Water Res Pl-Asce, 136, 59-71, 10.1061/(Asce)0733-9496(2010)136:1(59), 2010.

Castelletti, A., Pianosi, F., Quach, X., and Soncini-Sessa, R.: Assessing water reservoirs management and development in Northern Vietnam, Hydrol Earth Syst Sc, 16, 189-199, 10.5194/hess-16-189-2012, 2012.

Celeste, A. B., and Billib, M.: Evaluation of stochastic reservoir operation optimization models, Adv Water Resour, 32, 1429-1443, 10.1016/j.advwatres.2009.06.008, 2009.

Chang, F. J., and Chang, Y. T.: Adaptive neuro-fuzzy inference system for prediction of water level in reservoir, Adv Water Resour, 29, 1-10, 10.1016/j.advwatres.2005.04.015, 2006.

Cheng, C. T., Wang, S., Chau, K. W., and Wu, X. Y.: Parallel discrete differential dynamic programming for multireservoir operation, Environmental Modelling & Software, 57, 152-164, 10.1016/j.envsoft.2014.02.018, 2014.

Chu, J., Zhang, C., Fu, G., Li, Y., and Zhou, H.: Improving multi-objective reservoir operation optimization with sensitivity-informed dimension reduction, Hydrol Earth Syst Sc, 19, 3557-3570, 10.5194/hess-19-3557-2015, 2015.

Deb, K., Pratap, A., Agarwal, S., and Meyarivan, T.: A fast and elitist multiobjective genetic algorithm: NSGA-II, Ieee T Evolut Comput, 6, 182-197, 10.1109/4235.996017, 2002.

Duran, H., Puech, C., Diaz, J., and Sanchez, G.: Optimaloperation of multireservoir

https://doi.org/10.5194/hess-2019-586
Preprint. Discussion started: 17 March 2020

Hydrology and Earth System Sciences
Discussions

systems using an aggregation-decomposition approach, Ieee Transactions on Power Apparatus and Systems, 104, 2086-2092, 10.1109/Tpas.1985.318785, 1985.

Feng, Z. K., Niu, W. J., Cheng, C. T., and Wu, X. Y.: Optimization of hydropower system operation by uniform dynamic programming for dimensionality reduction, Energy, 134, 718-730, 10.1016/j.energy.2017.06.062, 2017.

Feng, Z. K., Niu, W. J., and Cheng, C. T.: Optimizing electrical power production of hydropower system by uniform progressive optimality algorithm based on two-stage search mechanism and uniform design, J Clean Prod, 190, 432-442, 10.1016/j.jclepro.2018.04.134, 2018a.

Feng, Z. K., Niu, W. J., Cheng, C. T., and Wu, X. Y.: Peak operation of hydropower system with parallel technique and progressive optimality algorithm, Int J Elec Power, 94, 267-275, 10.1016/j.ijepes.2017.07.015, 2018b.

Friedman, J. H.: Exploratory projection pursuit, J Am Stat Assoc, 82, 249-266, 10.2307/2289161, 1987.

Galelli, S., and Castelletti, A.: Tree-based iterative input variable selection for hydrological modeling, Water Resour Res, 49, 4295-4310, 10.1002/wrcr.20339, 2013.

Giuliani, M., Li, Y., Cominola, A., Denaro, S., Mason, E., and Castelletti, A.: A matlab toolbox for designing multi-objective optimal operations of water reservoir systems, Environ Modell Softw, 85, 293-298, 10.1016/j.envsoft.2016.08.015, 2016.

Glotic, A., and Zamuda, A.: Short-term combined economic and emission hydrothermal optimization by surrogate differential evolution, Appl Energ, 141, 42-56, 10.1016/j.apenergy.2014.12.020, 2015.

Goor, Q., Halleux, C., Mohamed, Y., and Tilmant, A.: Optimal operation of a multipurpose multireservoir system in the Eastern Nile River Basin, Hydrol Earth Syst Sc, 14, 1895-1908, 10.5194/hess-14-1895-2010, 2010.

He, S. K., Guo, S. L., Chen, K. B., Deng, L. L., Liao, Z., Xiong, F., and Yin, J. B.: Optimal impoundment operation for cascade reservoirs coupling parallel dynamic programming with importance sampling and successive approximation, Adv Water Resour, 131, 10.1016/j.advwatres.2019.07.005, 2019.

He, S. K., Guo, S. L., Yang, G., Chen, K. B., Liu, D. D., and Zhou, Y. L.: Optimizing operation rules of cascade reservoirs for adapting climate change, Water Resour Manag, 34, 101-120, 10.1007/s11269-019-02405-6, 2020.

Heever, S. A. V. D., and Grossmann, I. E.: An iterative aggregation/disaggregation approach for the solution of a mixed-integer nonlinear oilfield infrastructure planning model, Ind Eng Chem Res, 39, 1955-1971, 10.1021/ie9906619, 2000.

Jurasz, J., and Ciapala, B.: Integrating photovoltaics into energy systems by using a run-off-river power plant with pondage to smooth energy exchange with the power gird, Appl Energ, 198, 21-35, 10.1016/j.apenergy.2017.04.042, 2017.

Labadie, J. W.: Optimal operation of multireservoir systems: State-of-the-art review, J Water Res Plan Man, 130, 93-111, 10.1061/(Asce)0733-9496(2004)130:2(93), 2004.

Lauri, H., de Moel, H., Ward, P. J., Rasanen, T. A., Keskinen, M., and Kummu, M.: Future changes in Mekong River hydrology: impact of climate change and reservoir operation on discharge, Hydrol Earth Syst Sc, 16, 4603-4619, 10.5194/hess-16-4603-2012, 2012.

Lei, X. H., Zhang, J. W., Wang, H., Wang, M. N., Khu, S. T., Li, Z. J., and Tan, Q. F.: Deriving mixed reservoir operating rules for flood control based on weighted non-dominated sorting genetic algorithm II, J Hydrol, 564, 967-983, 10.1016/j.jhydrol.2018.07.075, 2018.

Li, H., Liu, P., Guo, S. L., Ming, B., Cheng, L., and Zhou, Y. L.: Hybrid two-stage stochastic methods using scenario-based forecasts for reservoir refill operations, J Water Res Plan Man, 144, 10.1061/(Asce)Wr.1943-5452.0001013, 2018.

Li, L. P., Liu, P., Rheinheimer, D. E., Deng, C., and Zhou, Y. L.: Identifying explicit formulation of operating rules for multi-reservoir systems using genetic programming, Water Resour Manag, 28, 1545-1565, 10.1007/s11269-014-0563-9, 2014a.

Li, X., Wei, J. H., Li, T. J., Wang, G. Q., and Yeh, W. W. G.: A parallel dynamic programming algorithm for multi-reservoir system optimization, Adv Water Resour, 67, 1-15, 10.1016/j.advwatres.2014.01.002, 2014b.

Liu, X. Y., Guo, S. L., Liu, P., Chen, L., and Li, X. A.: Deriving optimal refill rules for multi-purpose reservoir operation, Water Resour Manag, 25, 431-448, 10.1007/s11269-010-9707-8, 2011.

Lotfan, S., Ghiasi, R. A., Fallah, M., and Sadeghi, M. H.: ANN-based modeling and reducing dual-fuel engine's challenging emissions by multi-objective evolutionary algorithm NSGA-II, Appl Energ, 175, 91-99, 10.1016/j.apenergy.2016.04.099, 2016.

Ng, J. Y., Turner, S. W. D., and Galelli, S.: Influence of El Nino Southern Oscillation on global hydropower production, Environ Res Lett, 12, 10.1088/1748-9326/aa5ef8, 2017.

https://doi.org/10.5194/hess-2019-586
Preprint. Discussion started: 17 March 2020

Hydrology and Earth System Sciences Discussions

Paredes, J., and Lund, J. R.: Refill and drawdown rules for parallel reservoirs: Quantity and quality, Water Resour Manag, 20, 359-376, 10.1007/s11269-006-0325-4, 2006.

Saad, M., Turgeon, A., Bigras, P., and Duquette, R.: Learning disaggregation technique for the operation of long-term hydroelectric power-systems, Water Resour Res, 30, 3195-3202, 10.1029/94wr01731, 1994.

Shaw, A. R., Sawyer, H. S., LeBoeuf, E. J., McDonald, M. P., and Hadjerioua, B.: Hydropower optimization using artificial neural network surrogate models of a high-fidelity hydrodynamics and water quality model, Water Resour Res, 53, 9444-9461, 10.1002/2017wr021039, 2017.

Tan, Q. F., Wang, X., Wang, H., Wang, C., Lei, X. H., Xiong, Y. S., and Zhang, W.: Derivation of optimal joint operating rules for multi-purpose multi-reservoir water-supply system, J Hydrol, 551, 253-264, 10.1016/j.jhydrol.2017.06.009, 2017.

Turgeon, A.: Optimal operation of multi-reservoir power-systems with stochastic inflows, Water Resour Res, 16, 275-283, 10.1029/WR016i002p00275, 1980.

Valdes, J. B., Montbrundifilippo, J., Strzepek, K. M., and Restrepo, P. J.: Aggregation-disaggregation approach to multireservoir operation, J Water Res Pl-Asce, 118, 423-444, 10.1061/(Asce)0733-9496(1992)118:4(423), 1992.

Wang, X. M., Zhou, J. Z., Ouyang, S., and Li, C. L.: Research on joint impoundment dispatching model for cascade reservoir, Water Resour Manag, 28, 5527-5542, 10.1007/s11269-014-0820-y, 2014.

Xie, M. F., Zhou, J. Z., Li, C. L., and Zhu, S.: Long-term generation scheduling of Xiluodu and Xiangjiaba cascade hydro plants considering monthly streamflow forecasting error, Energ Convers Manage, 105, 368-376, 10.1016/j.enconman.2015.08.009, 2015.

Xu, B., Boyce, S. E., Zhang, Y., Liu, Q., Guo, L., and Zhong, P. A.: Stochastic programming with a joint chance constraint model for reservoir refill operation considering flood risk, J Water Res Plan Man, 143, 10.1061/(Asce)Wr.1943-5452.0000715, 2017.

Yan, D. H., Wang, H., Li, H. H., Wang, G., Qin, T. L., Wang, D. Y., and Wang, L. H.: Quantitative analysis on the environmental impact of large-scale water transfer project on water resource area in a changing environment, Hydrol Earth Syst Sc, 16, 2685-2702, 10.5194/hess-16-2685-2012, 2012.

Yeh, W. W. G.: Reservoir management and operations models - a State-of-the-Art review, Water Resour Res, 21, 1797-1818, 10.1029/WR021i012p01797, 1985.

Zhang, J. W., Wang, X., Liu, P., Lei, X. H., Li, Z. J., Gong, W., Duan, Q. Y., and Wang, H.: Assessing the weighted multi-objective adaptive surrogate model optimization to derive large-scale reservoir operating rules with sensitivity analysis, J Hydrol, 544, 613-627, 10.1016/j.jhydrol.2016.12.008, 2017.

Zhang, J. W., Li, Z. J., Wang, X., Lei, X. H., Liu, P., Feng, M. Y., Khu, S. T., and Wang, H.: A novel method for deriving reservoir operating rules based on flood classification-aggregation-decomposition, Journal of Hydrology, 568, 722-734, 10.1016/j.jhydrol.2018.10.032, 2019.

Zhang, R., Zhou, J. Z., Zhang, H. F., Liao, X., and Wang, X. M.: Optimal operation of large-scale cascaded hydropower systems in the upper reaches of the Yangtze river,

https://doi.org/10.5194/hess-2019-586
Preprint. Discussion started: 17 March 2020

Hydrology and Earth System Sciences
Discussions

China, J Water Res Plan Man, 140, 480-495, 10.1061/(Asce)Wr.1943-5452.0000337, 2014.

Zhao, T. T. G., Cai, X. M., Lei, X. H., and Wang, H.: Improved dynamic programming for reservoir operation optimization with a concave objective function, J Water Res Pl-Asce, 138, 590-596, 10.1061/(Asce)Wr.1943-5452.0000205, 2012.

Zhou, Y. L., Guo, S. L., Xu, C. Y., Liu, P., and Qin, H.: Deriving joint optimal refill rules for cascade reservoirs with multi-objective evaluation, J Hydrol, 524, 166-181, 10.1016/j.jhydrol.2015.02.034, 2015.

Zhou, Y. L., Guo, S. L., Chang, F. J., and Xu, C. Y.: Boosting hydropower output of mega cascade reservoirs using an evolutionary algorithm with successive approximation, Appl Energ, 228, 1726-1739, 10.1016/j.apenergy.2018.07.078, 2018.

https://doi.org/10.5194/hess-2019-586
Preprint. Discussion started: 17 March 2020

Hydrology and Earth System Sciences Discussions

List of Table

Table 1 Impounding times and characteristic parameters of the 30-reservoir system in seven pools (A-G) in the upper Yangtze River

Table 2 The sum storage capacity of $SS_{i,n}(t)$ of all reservoirs in the same pool at different periods (billion m^3)

https://doi.org/10.5194/hess-2019-586
Preprint. Discussion started: 17 March 2020

Table 1

Impounding times and characteristic parameters of the 30-reservoir system in seven pools (A-G) in the upper Yangtze River

Pool	Reservoir	Initial time of impoundment		End time of impoundment (COR, PSO)	Annual top of buffer pool (m)	Top of conservation pool (m)	Total storage capacity (billion m^3)	Storage capacity for flood control (billion m^3)	Installed hydropower capacity (GW)
		COR[a]	PSO[b]						
Pool A[c] (middle Jinsha River)	(A1) LY	Aug. 1st	Aug.1st	Sep. 30th	1605	1618	0.81	0.17	2.40
	(A2) AH	Aug. 1st	Aug.1st	Sep. 30th	1493.3	1504	0.89	0.22	2.00
	(A3) JAQ	Aug. 1st	Aug.1st	Sep. 30th	1410	1418	0.91	0.16	2.40
	(A4) LKK	Aug. 1st	Aug.1st	Sep. 30th	1289	1298	0.56	0.13	1.80
	(A5) LDL	Aug. 1st	Aug.1st	Sep. 30th	1212	1223	1.72	0.56	2.16
	(A6) GYY	Oct. 1st	Sep.20th	Oct. 31st	1128.8	1134	2.25	0.25	3.00
Pool B (Yalong River)	(B1) LHK	Aug. 1st	Aug. 1st	Sep. 30th	2845	2865	10.15	2.00	3.00
	(B2) JP	Aug. 1st	Aug. 1st	Sep. 30th	1859	1880	7.99	1.60	3.60
	(B3) ET	Aug. 1st	Aug. 1st	Sep. 30th	1190	1200	5.80	0.90	3.30
Pool C (Downstream Jinsha River)	(C1)WDD	Aug. 10st	Aug.1st	Sep. 10th	952	975	3.94	2.44	10.20
	(C2) BHT	Aug. 10st	Aug.1st	Sep. 30th	785	825	20.60	7.50	16.00
	(C3) XLD	Sep. 1st	Aug. 20th	Sep. 30th	560	600	12.67	4.65	13.86
	(C4) XJB	Sep. 10th	Aug. 20th	Sep. 30th	370	380	5.16	0.90	7.75
Pool D (Min River)	(D1) ZPP	Oct. 1st	Sep.20th	Oct. 31st	850	877	1.11	0.17	0.76
	(D2) XEX	Oct. 1st	Sep.20th	Oct. 31st	3105	3120	2.80	0.87	0.54
	(D3) SJK	Oct. 1st	Sep.20th	Oct. 31st	2480	2500	2.90	0.66	2.00
	(D4) PBG	Oct. 1st	Sep.20th	Oct. 31st	841	850	5.33	0.73	3.60

Pool E (Jialing River)	(E1) BK	Oct. 1st	Sep.20th	Oct. 31st	695	704	0.22	0.10	0.30
	(E2) BZS	Oct. 1st	Sep.20th	Oct. 31st	583	588	2.55	0.28	0.70
	(E3) TZK	Sep. 1st	Aug. 20th	Sep. 30th	447	458	4.07	1.44	1.10
	(E4) CJ	Sep. 1st	Aug. 20th	Sep. 30th	200	203	2.22	0.20	0.50
Pool F (Wu River)	(F1) HJD	Sep. 1st	Aug. 20th	Sep. 30th	1138	1140	4.95	0.15	0.60
	(F2) DF	Sep. 1st	Aug. 20th	Sep. 30th	968	970	1.02	0.04	0.57
	(F3) WJD	Sep. 1st	Aug. 20th	Sep. 30th	756	760	2.30	0.18	1.25
	(F4) GPT	Sep. 1st	Aug. 20th	Sep. 30th	628.1	630	6.45	0.20	3.00
	(F5) SL	Sep. 1st	Aug. 20th	Sep. 30th	435	440	1.59	0.18	1.05
	(F6) ST	Sep. 1st	Aug. 20th	Sep. 30th	357	365	0.92	0.21	1.12
	(F7) PS	Sep. 1st	Aug. 20th	Sep. 30th	287	293	1.47	0.23	1.75
Pool G (TGR-GZB)	(G1) TGR	Sep. 10th	Aug. 20th	Oct. 31st	145	175	45.07	22.15	22.50
	(G2) GZB	-	-	-	-	66	1.58	-	2.72

Note:

(a) COR: Conventional Operating Rule; (b) PSO: Parameterization Simulation Optimization.

https://doi.org/10.5194/hess-2019-586
Preprint. Discussion started: 17 March 2020

Hydrology and Earth System Sciences
Discussions

Table 2

The sum storage capacity $SS_{i,n}(t)$ of all reservoirs in the same pool at different periods (billion m^3)

Pool	Aug.10th	Aug.20th	Aug.31st	Sep.10th	Sep.20th	Sep.30th	Oct.10th	Oct.20th	Oct.31st
A	5.40	5.73	6.16	6.29	6.41	6.51	6.51	6.51	6.51
B	20.05	21.74	22.65	23.68	23.68	23.68	23.68	23.68	23.68
C	29.21	33.50	35.95	38.85	41.13	41.40	41.40	41.40	41.40
D	9.29	9.29	9.61	9.94	10.38	11.16	11.44	11.66	11.66
E	4.82	4.97	5.52	6.34	6.40	6.42	6.53	6.56	6.56
F	15.37	15.71	16.04	16.26	16.26	16.26	16.26	16.26	16.26
G	18.12	19.75	21.51	24.76	30.04	32.60	39.31	39.31	39.31

Note: the meaning of $SS_{i,n}(t)$ is referred in Eq. (3).

https://doi.org/10.5194/hess-2019-586
Preprint. Discussion started: 17 March 2020

Hydrology and Earth System Sciences Discussions
Open Access EGU

List of Figures

https://doi.org/10.5194/hess-2019-586
Preprint. Discussion started: 17 March 2020

Hydrology and Earth System Sciences
Open Access
Discussions

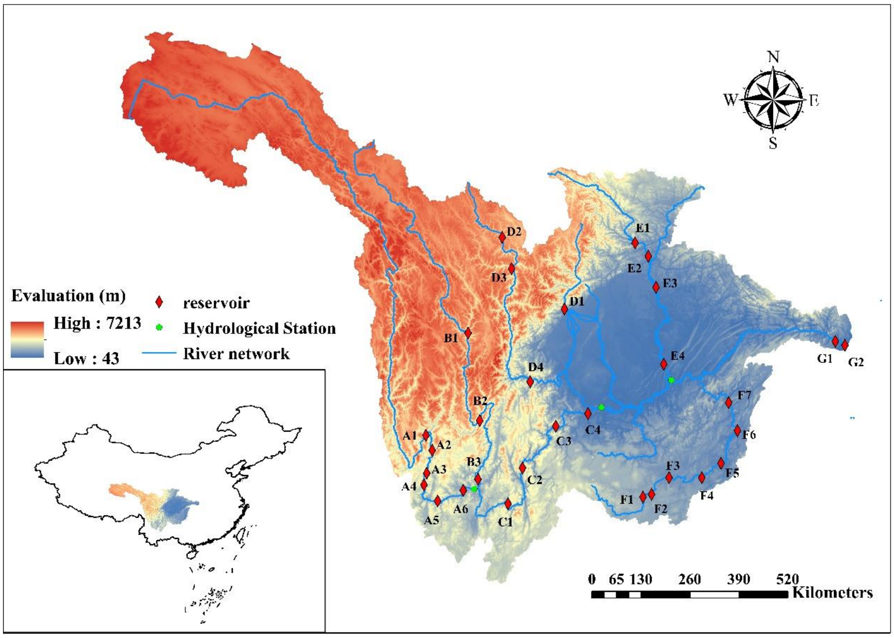

Fig. 1a Geographic distribution of the 30-reservoir system

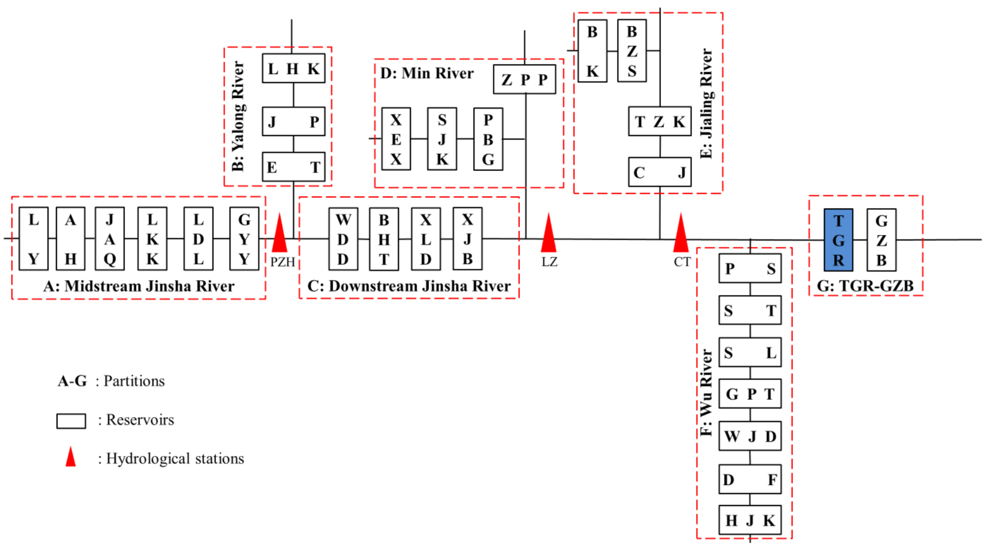

Fig. 1b Schematic diagram of the 30-reservoir system

Fig. 1 Location information of the mixed 30 reservoirs in the upper Yangtze River

https://doi.org/10.5194/hess-2019-586
Preprint. Discussion started: 17 March 2020

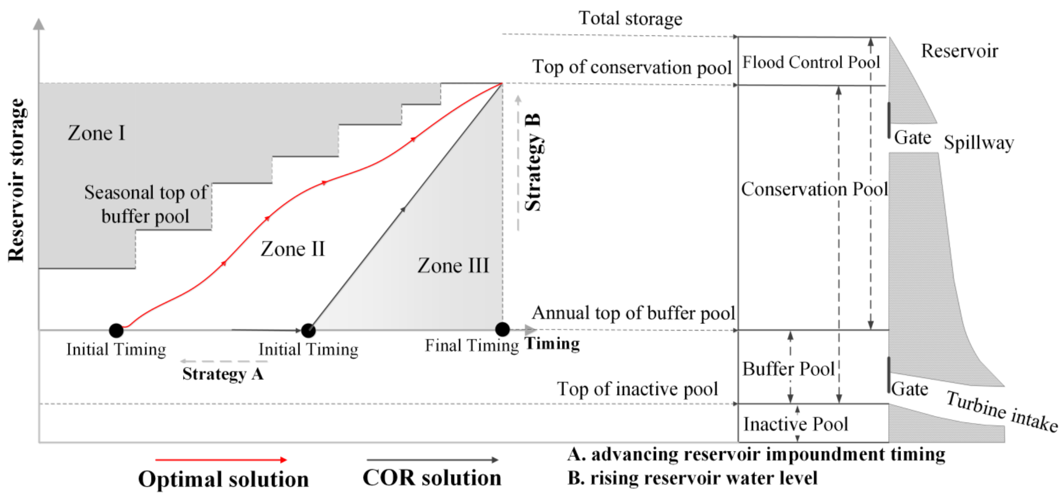

Fig. 2 The schematic diagram of two activate strategies for advanced impoundment

https://doi.org/10.5194/hess-2019-586
Preprint. Discussion started: 17 March 2020

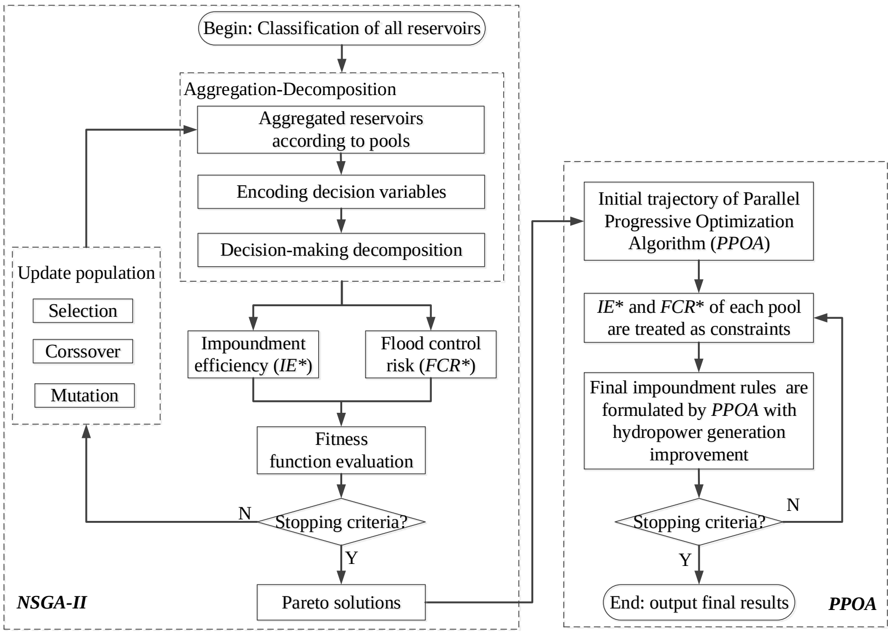

Fig. 3 Flowchart of deriving joint impoundment rules for the large-scale reservoir system

https://doi.org/10.5194/hess-2019-586
Preprint. Discussion started: 17 March 2020

Hydrology and Earth System Sciences Discussions
Open Access
EGU

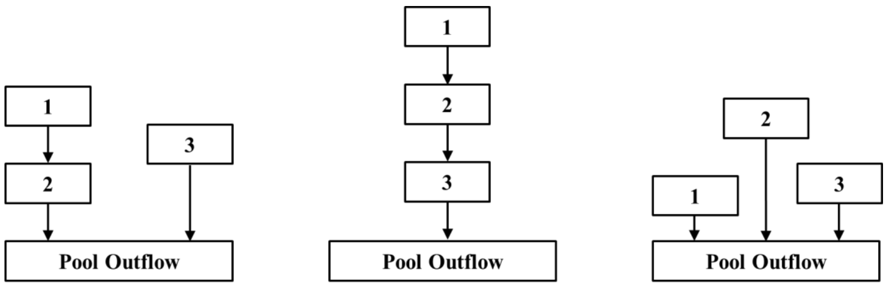

(a) mixed-connected case (b) series case (c) parallel case

Fig. 4 Three general topological cases of reservoir location

https://doi.org/10.5194/hess-2019-586
Preprint. Discussion started: 17 March 2020

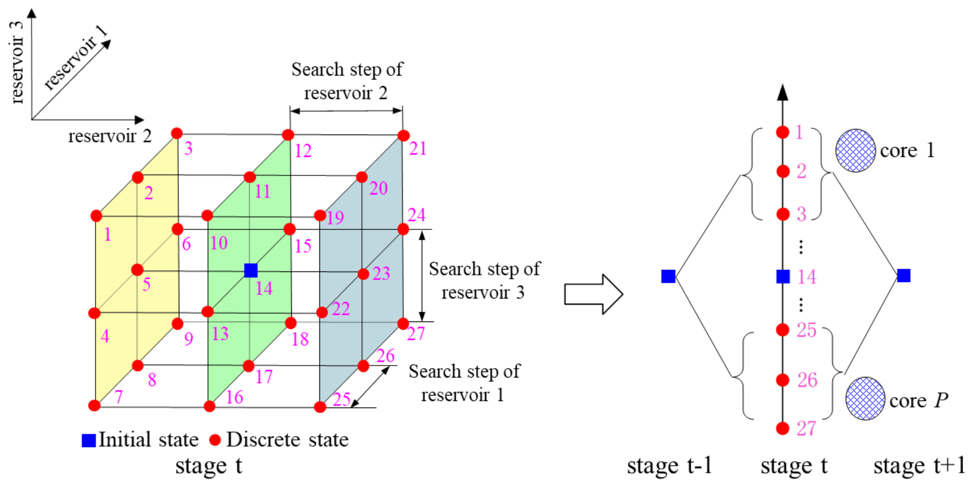

Fig. 5 Sketch map of the PPOA algorithm for a sub-problem with 3-reservoir and 3 levels per reservoir

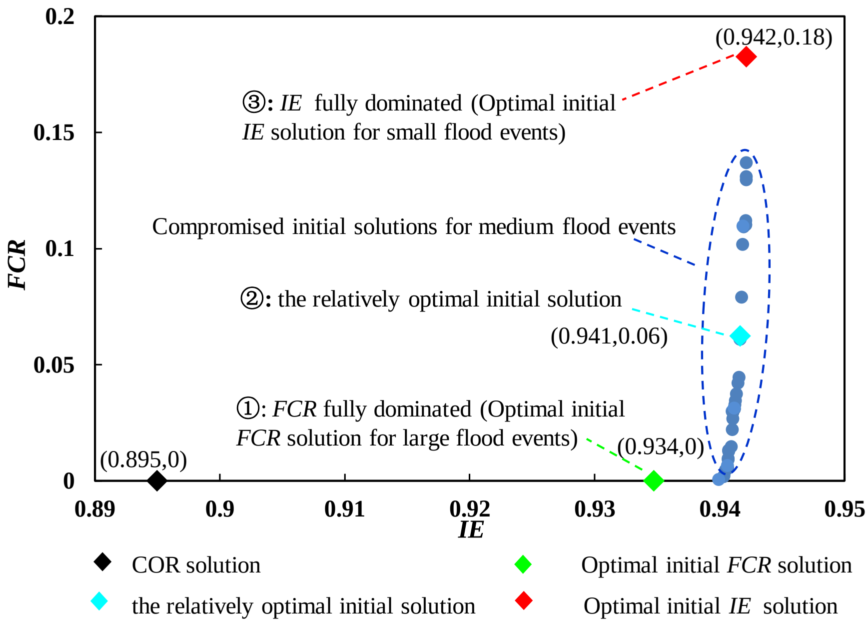

Fig. 6 Comparison of the *IE* and *FCR* results of different initial optimal solutions

https://doi.org/10.5194/hess-2019-586
Preprint. Discussion started: 17 March 2020

Hydrology and Earth System Sciences
Open Access
Discussions

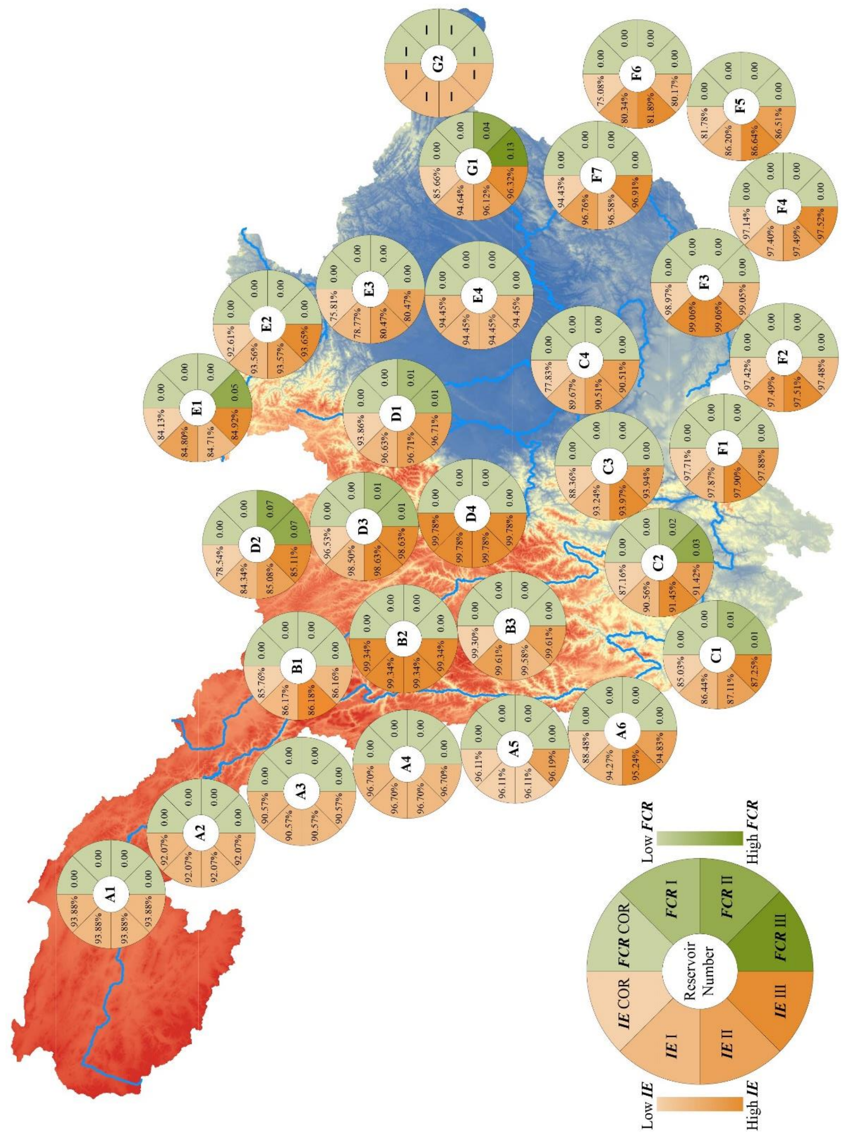

Fig. 7 Spatial varieties of *IE* and *FCR* of each reservoir relative to the different optimal impoundment rules

https://doi.org/10.5194/hess-2019-586
Preprint. Discussion started: 17 March 2020

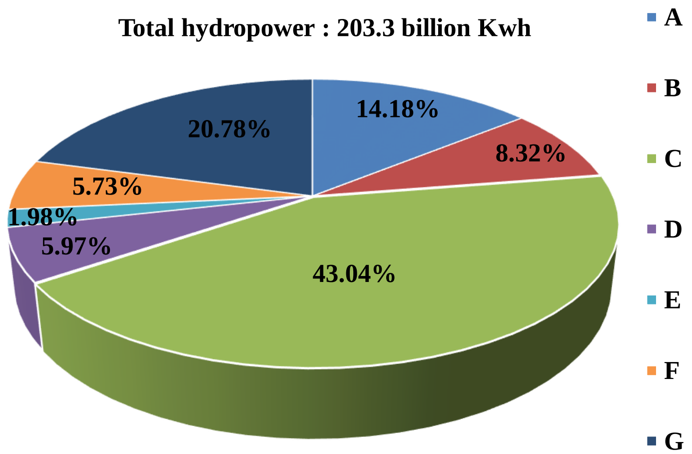

Fig. 8 Hydropower proportion of each pool based on the COR rule

https://doi.org/10.5194/hess-2019-586
Preprint. Discussion started: 17 March 2020

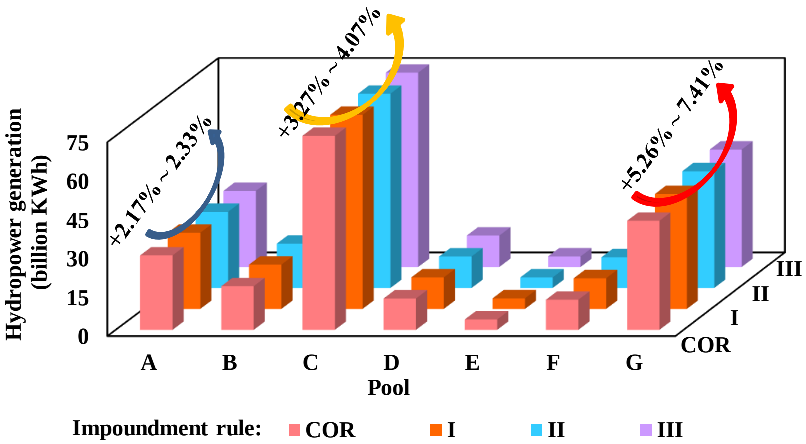

Fig. 9 The hydropower results of the 30 reservoirs in seven pools for different impoundment rules

https://doi.org/10.5194/hess-2019-586
Preprint. Discussion started: 17 March 2020

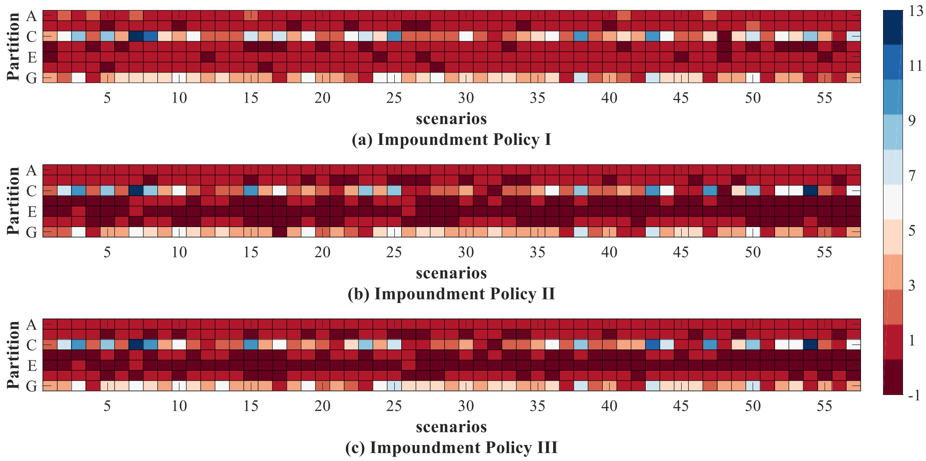

743 **Fig. 10** Hydropower increment of seven pools (A-G) for three optimal impoundment
744 policies compared to the COR rule in different streamflow scenarios (Unit: billion kWh)

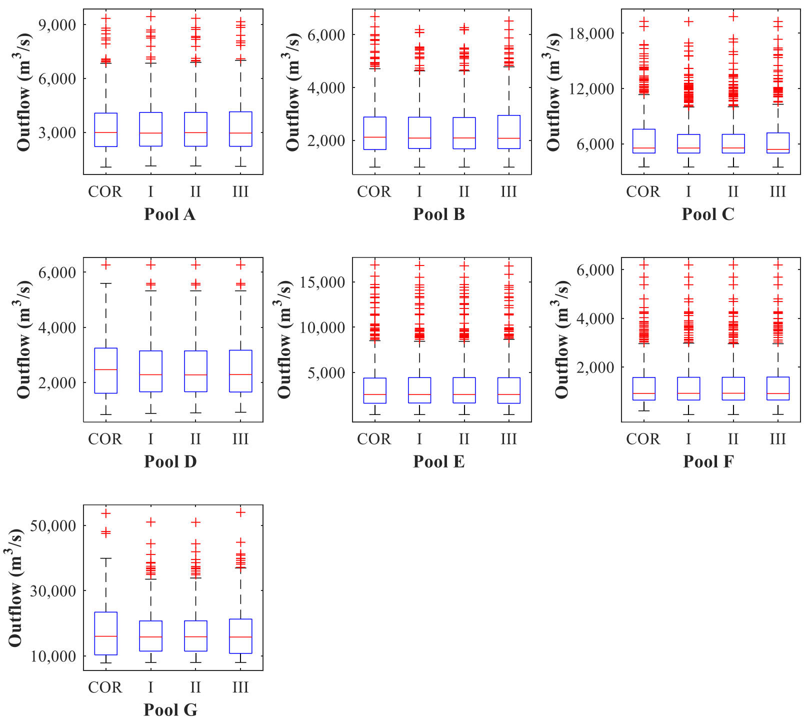

Fig. 11 Outflow distribution of all Pools (A~F) during the impoundment period

https://doi.org/10.5194/hess-2019-586
Preprint. Discussion started: 17 March 2020

Hydrology and Earth System Sciences
Discussions

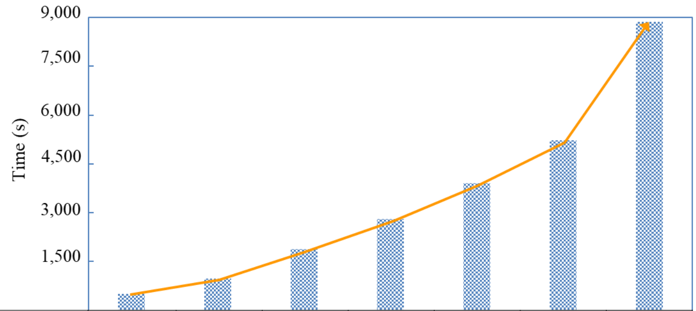

Pool	A	A~B	A~C	A~D	A~E	A~F	A~G
Number of reservoirs	6	9	13	17	21	28	30
Time (s)	499	975	1884	2806	3909	5224	8868

Fig. 12 Computational efficiency for different numbers of pools